Thermoelectric properties of Pb doped $[Ca_2CoO_{3.1}]_{0.62}CoO_2$

H. Nakatsugawa , H. M. Jeong, R. H. Kim and N. Gomi
Graduate school of Engineering, Yokohama National University,
79-5 Tokiwadai, Hodogaya-ku, Yokohama 240-8501, Japan
E-mail: naka@ynu.ac.jp, TEL: +81-45-339-3854, FAX: +81-45-331-6593

Abstract

We have prepared polycrystalline specimens of $[(Ca_{1-x}Pb_x)_2CoO_{3.1}]_{0.62}CoO_2$ $(0 \leqq x \leqq 0.03)$ using the conventional solid-state reaction method, and investigated the Pb substitution effect on the TE properties. With the Pb substitution, both the electrical resistivity and Seebeck coefficient do not change drastically. This is attributed to the carrier concentration. Seebeck and Hall coefficient measurements reveal that the major charge carriers in the samples are holes, however, the carrier concentration does not change drastically with increasing x. The magnetic susceptibility measurements also show that Pb ions take divalent state in the rock salt type $[Ca_2CoO_3]$ block layer. The valence state of Co ions in the CdI_2 type $[CoO_2]$ sheet was 3.1+ and that of Co ions in the block layer was 3.6+. The dimensionless figure of merit for the x = 0 sample at room temperature was 0.02, which is approximately equal to the corresponding values of a polycrystalline sample of $NaCo_2O_4$.

1. Introduction

Since the discovery of large thermoelectric power in the layered compounds $NaCo_2O_4$ [1] and $Ca_3Co_4O_9$ [2-4], misfit-layered cobalt oxides particularly have attracted much interest as candidates for thermoelectric (TE) materials. The Crystal structure of $Ca_3Co_4O_9$ consists of an alternate stack of a distorted three-layered rock salt (RS)-type Ca_2CoO_3 block layer (BL) and a CdI_2-type CoO_2 conducting sheet parallel to the c-axis.[3, 5, 6] The CdI_2-type CoO_2 subsystem and the RS-type BL subsystem have common a- and c-axes and beta angles. Owing to the size difference between the RS-type BL and the CoO_2 sheet, however, the compound has an incommensurate periodicity parallel to the b-axis. The resulting structural formula becomes $[Ca_2CoO_{3-y}]_pCoO_2$, where $p = b_{CoO_2}/b_{Ca_2CoO_3}$ and y is an oxygen nonstoichiometry. The chemical formula can be approximately represented as $Ca_{1.24}Co_{1.62}O_{3.86}$. Throughout this paper, we will use the structural formula of the compound instead of the chemical formula. Such an anisotropic structure of the compound is believed to be favorable in realizing large Seebeck coefficient, S, and low thermal conductivity, κ, necessary for good TE compounds. The RS-type BL can be regarded as a charge reservoir, which introduces hole carriers into the CoO_2 sheet. In addition, a CoO_2 triangular lattice in the CoO_2 sheet should play an important role for realizing low electrical resistivity, ρ, namely, large TE power factor.

The polycrystalline $Ca_3Co_4O_9$ sample typically exhibits S~130 μ V/K, $\rho \sim$ 15m Ω cm and $\kappa \sim$ 1.0W/mK at room temperature.[4] For practical use, an appreciable decrease in ρ must be achieved because ρ at room temperature is about one order of magnitude higher than that of Bi_2Te_3-based TE materials. Much effort has been devoted to decrease ρ while

maintaining a large S and low κ, through partial substitutions for Ca atoms in the RS-type BL. The optimization of the valence state of the RS-type BL is a key issue to maximize the TE properties because ρ and S are highly dependent on the nominal valence state of Co ions in the CoO_2 sheet. In fact, Li *et al.*[7] and Funahashi *et al.*[8] reported a marked increase in their TE performance by partial substitution of Bi for Ca. However, no effect of the Pb-substituted samples has been reported. We have employed a high-resolution neutron powder diffraction technique to investigate the modulated crystal structure of the Pb doped $[Ca_2CoO_{3.1}]_{0.62}CoO_2$ polycrystalline samples. In this study, we report the effect of partial substitution of Pb^{2+} for Ca^{2+} on the crystal structure and TE properties.

2. Experiment

Polycrystalline specimens of $[(Ca_{1-x}Pb_x)_2CoO_{3.1}]_{0.62}CoO_2$ $(0 \leqq x \leqq 0.03)$ were prepared by the conventional solid-state reaction method starting from powder mixture of $CaCO_3$ (99.9%), PbO (99.9%) and Co_3O_4 (99.9%) with a stoichiometric cation ratio. After calcination in air at 920℃ for 12h, the calcined powders were pressed into pellets with 13mm $\phi \times$ 1mm in dimension and sintered in pure flowing oxygen gas at 920℃ for 20h. The obtained well-crystallized single-phase samples were annealed in pure flowing oxygen gas at 700℃ for 12h and then quenched into distilled water to control oxygen nonstoichiometry.[9] Through the synthesis, the nominal b-axis ratio was fixed at about 0.62.

Neutron powder diffraction (ND) data were collected at room temperature using the Kinken powder diffractometer for high efficiency and high resolution measurements (HERMES) of Institute for Materials Research (IMR), Tohoku University, installed at the JRR-3M reactor in Japan Atomic Energy Research Institute (JAERI), Tokai.[10] Neutrons with a wavelength of 1.8265 Å were obtained by the 331 reflection of the Ge monochromator. The ND data were collected on thoroughly ground powders by a multiscanning mode in the 2 θ range from 3.0° to 153.9° with a step width of 0.1° and were analyzed using a Rietveld refinement program, PREMOS 91 [11], adopting a superspace group of *C2/m(1p0)s0*, where $[CoO_2]$ subsystem has *C2/m* symmetry while $[Ca_2CoO_{3.1}]$ subsystem has *C2₁/m* symmetry. The crystal structures and interatomic distance plots were obtained with the use of PRJMS and MODPLT routines, respectively; both were implemented in the PREMOS 91 package.

Measurements of electrical resistivity, Seebeck coefficient and Hall coefficient were carried out in temperature range from 80K to 380K. Measurements of thermal conductivity were carried out at room temperature. Measurements of magnetic susceptibility were carried out in the temperature range from 2K to 350K. The electrical resistivity, ρ , was

measured by the van der Pauw technique with a current of 10 mA in He atmosphere. The thermal conductivity, κ, was calculated from $\kappa = A \cdot C \cdot D$, where A is the thermal diffusivity, C is the specific heat and D is the measured sample density. The thermal diffusivity was measured using the laser flash method (ULVAC, TC-3000) at room temperature. The Hall coefficient R_H measurement was performed on flat square pieces of materials with a current of 100 mA in a magnetic field of 0.85T by the van der Pauw technique. The Hall carrier concentration n was determined from R_H using $n = 1/eR_H$, where e is the electron charge, assuming a scattering factor equal to 1 and a single carrier model. The Hall mobility, μ, was determined from ρ and R_H using $\mu = R_H/\rho$. The magnetic susceptibility was measured using a superconducting quantum interference device (SQUID) magnetometer (Quantum Design, MPMS) under the zero-field cooling (ZFC) and field cooling (FC) conditions in a magnetic field of 10 Oe.

3. Results And Discussion

Fig.1 shows the temperature dependence of the electrical resistivity of the specimens with $[(Ca_{1-x}Pb_x)_2CoO_{3.1}]_{0.62}CoO_2$ ($0 \leqq x \leqq 0.03$) measured at the temperature range from 80K to 380K. All the samples show metallic $\rho(T)$ behavior down to around 100K. With further decrease in the temperature, the samples turn to be semiconducting behavior due to the occurrence of the spin-density-wave (SDW) transition. Sugiyama et al.[12] have suggested that the polycrystalline $Ca_3Co_4O_9$ sample exhibits the SDW transition at around 100K, and the Co ions in the RS-type BL play an important role in including the SDW transition. The electrical resistivity at room temperature is summarized in Table 1. For $x = 0$ and 0.02 samples, the ρ values are 17.3×10^{-3} and $16.7 \times 10^{-3} \Omega cm$, respectively at room temperature.

The temperature dependence of the Seebeck coefficient S of samples with $[(Ca_{1-x}Pb_x)_2CoO_{3.1}]_{0.62}CoO_2$ ($0 \leqq x \leqq 0.03$) is presented in Fig.2. The S values are all positive, mean that the major charge carriers in the compound are holes, i.e., p-type conduction. It can be seen clearly that at the temperatures above 100K the Seebeck coefficient of $[(Ca_{1-x}Pb_x)_2CoO_{3.1}]_{0.62}CoO_2$ compounds shows weak temperature dependence. The Seebeck coefficient at room temperature is summarized in Table 1. The effect of the Pb substitution on the S values could be interpreted by the framework of the model which was proposed to explain the large Seebeck coefficient of the $NaCo_2O_4$. In that model, the Seebeck coefficient can be estimated by using the modified Heikes formula[13]:

$$S = -\frac{k_B}{e} \ln\left[\frac{g_3}{g_4}\frac{c}{1-c}\right],$$

where g_3, g_4 are the number of the degenerated configurations of the Co^{3+} and Co^{4+} states in the CoO_2 sheet while $c = Co^{4+}/Co$ is the fraction of Co^{4+} holes on the Co sites in the $[CoO_2]$ subsystem. Since the electronic configuration of Co^{3+} and Co^{4+} ion is the low spin state, the number of the degenerated configurations of the Co^{3+} and Co^{4+} states in the CoO_2 sheet is $g_3=1$ and $g_4=6$, respectively. Thus according to

the above formula, the S values would stay constant without the change in c value. In the present study, the substitution of divalent Pb^{2+} for divalent Ca^{2+} would keep the hole (Co^{4+}) concentrations. Despite the increase in the Pb content, therefore, $[(Ca_{1-x}Pb_x)_2CoO_{3.1}]_{0.62}CoO_2$ compounds shows similar S.
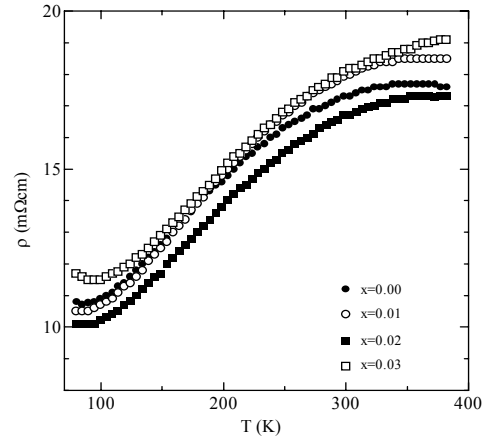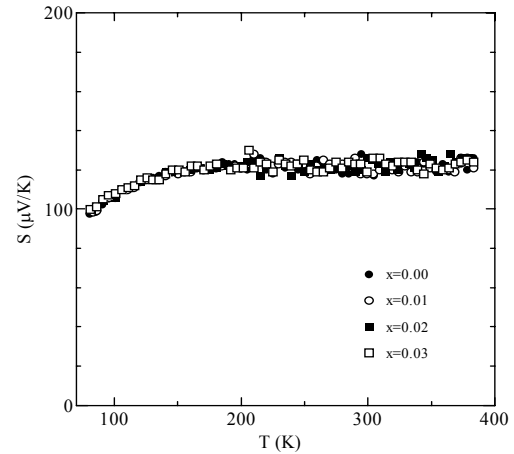

Fig.1 Temperature dependence of resistivity ρ.

Fig.2 Temperature dependence of Seebeck coefficient S.

The TE power factor, S^2/ρ, of $[(Ca_{1-x}Pb_x)_2CoO_{3.1}]_{0.62}CoO_2$ ($0 \leqq x \leqq 0.03$) values at room temperature are summarized in Table 1. The sample with $x = 0.02$ exhibits largest TE power factor, $0.95 \times 10^{-4} W/mK^2$ at room temperature. With decreasing temperature, the sample shows a broad maximum at around $100 - 150K$. With further decrease in temperature, the S^2/ρ value decreases steadily. Since the Seebeck coefficient $S(T)$ behavior does not change very much as shown in Fig.2, the change in the TE power factor is primarily due to the change in the electrical resistivity.

Fig.3 shows the temperature dependence of the Hall coefficient of the samples with $[(Ca_{1-x}Pb_x)_2CoO_{3.1}]_{0.62}CoO_2$ ($0 \leqq x \leqq 0.03$) measured at the temperature range from 80K to 380K. All the samples show a positive value of R_H and similar values. Hall coefficient measurements reveal that the major charge carriers in the samples are holes. The signs of Hall coefficient were consistent with those of Seebeck coefficient. Electrical resistivity ρ, Hall coefficient R_H, Hall carrier concentration $n = 1/eR_H$, Hall mobility $\mu = R_H/\rho$ and power

factor S^2/ρ at room temperature are summarized in Table 1. The Hall carrier concentration of $[(Ca_{1-x}Pb_x)_2CoO_{3.1}]_{0.62}CoO_2$ $(0 \leqq x \leqq 0.03)$ have the magnitude of $5.5 \sim 5.7 \times 10^{20} cm^{-3}$ at room temperature. For $x = 0$ and 0.02 samples, the μ values are 0.64 and 0.66 cm^2/Vs, respectively at room temperature.
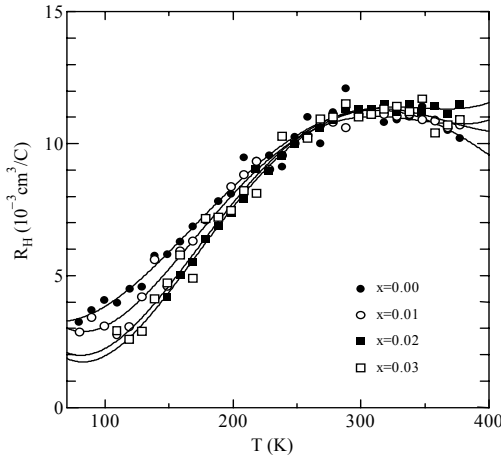

Fig.3 Temperature dependence of Hall coefficient R_H.

The thermal conductivity κ of the sample with $x = 0$ at room temperature is calculated from $\kappa = A \cdot C \cdot D$, where $A = 6.28 \times 10^{-3} cm^2/s$ is thermal diffusivity, $C = 0.616 J/gK$ is specific heat and $D = 3.2 g/cm^3$ is the measured density. The value of κ at room temperature is 1.24W/mK, which is approximately 30% smaller than the value reported for $NaCo_2O_4$ at room temperature[14]. Thermal conductivity can be expressed by the sum of lattice component κ_L and electronic component κ_e as $\kappa = \kappa_L + \kappa_e$. The κ_e value can be estimated from Wiedemann-Franz's law as $\kappa_e = LT/\rho$, where L is the Lorentz number ($L = 2.44 \times 10^{-8} V^2/K^2$ for free electrons). At room temperature, the electronic component κ_e for all the samples is $0.04 W/mK$. Hence, for $x = 0$ sample, the estimated lattice component κ_L is $1.20W/mK$. Thermal diffusivity A, the measured density D, the specific heat C, the electron thermal conductivity κ_e and the lattice component κ_L at room temperature are summarized in Table 1. The dimensionless TE figure of merit ZT is calculated from the equation, $ZT = S^2T/\rho\kappa$. As summarized in Table 1, the ZT value for the $x = 0$ sample at room temperature is 0.02, which is approximately equal to the corresponding values of a polycrystalline sample of $NaCo_2O_4$[14], suggesting that $[(Ca_{1-x}Pb_x)_2CoO_{3.1}]_{0.62}CoO_2$ $(0 \leqq x \leqq 0.03)$ are another candidate for TE compounds.

Lead ions take either the 2+ or 4+ state in the RS-type BL. In the case of Pb^{2+}, the ionic radius is 1.29 Å [15] (coordination number, CN=8). As the ionic radius of Ca^{2+} is nearly equal (1.12 Å, CN=8), it is reasonable to consider that Ca^{2+} is partially replaced by Pb^{2+}. On the other hand, lead ions must be Pb^{4+} in the Co2 site because some of the Co2-O bond lengths, i.e., Co2-O3 bond lengths are as short as 1.8 Å. To account for such a short bond length, the major part of Pb ions

should be in the tetravalent state with an ionic radius of 0.775 Å (CN=6), although this ionic radius is much larger than that of low spin Co^{3+} (0.545 Å, CN=6). However, it is not possible to substitute Pb^{4+} of the Co2 site because the Co2-O3 modulation does not change with increasing x as shown in Fig.4. Thus, Pb ions take divalent state in the RS-type BL.
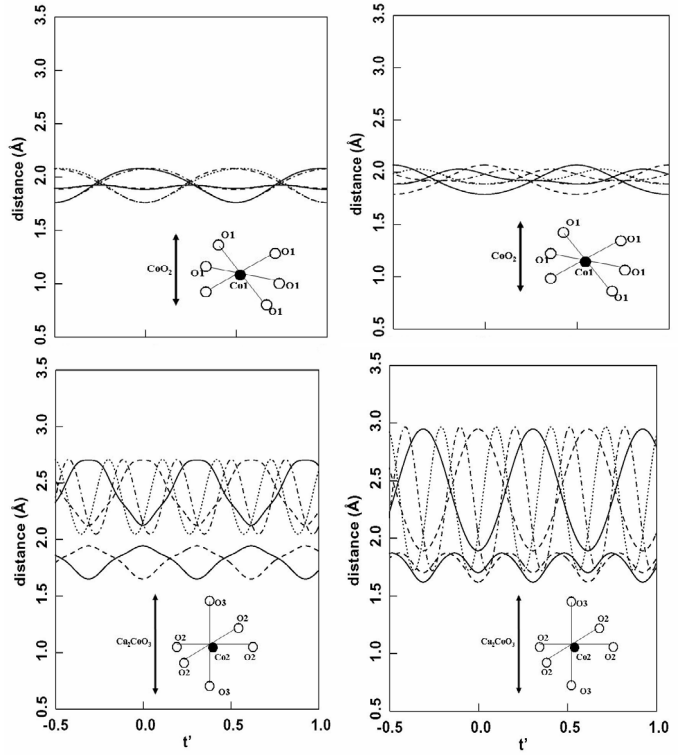

Fig.4 Co-O distances : $x = 0$ (left) and $x = 0.02$ (right).

Let us evaluate the valence state of Co ions in $[(Ca_{1-x}Pb_x)_2CoO_{3.1}]_{0.62}CoO_2$ $(0 \leqq x \leqq 0.03)$ assuming that the valence state of lead ions are Pb^{2+}. Sugiyama *et al.*[12] have suggested that the polycrystalline $Ca_3Co_4O_9$ sample exhibits ferromagnetic transition at $T_C = 19K$, due to an antiferromagnetic (AF) order of the Co1 and Co2 sublattices. Figure 5 represents the temperature dependence of the inverse-magnetic susceptibility, $(\chi - \chi_0)^{-1}$, of the $x = 0.02$ sample measured the zero-field cooling (ZFC) condition in a magnetic field of 10 Oe. As shown in Fig.5, the sample exhibits a positive curvature characteristic of ferromagnetic compound. On the basis of the mean-field-approximation theory.[16] The effective magnetic moment of each Co site is then determined using the obtained Curie constant. From ^{59}Co NMR studies of $NaCo_2O_4$[17], both Co1 and Co2 site consist of a mixture of low-spin Co^{3+} ($S=0$) and Co^{4+} ($S=1/2$). Hence, the average valence state of each Co ion (n_m) can be directly derived from $S_m = n_m/2$ using the formula: $\mu_{eff} = 2\sqrt{S_m(S_m + 1)}$.

Table 1. Thermoelectric properties at room temperature

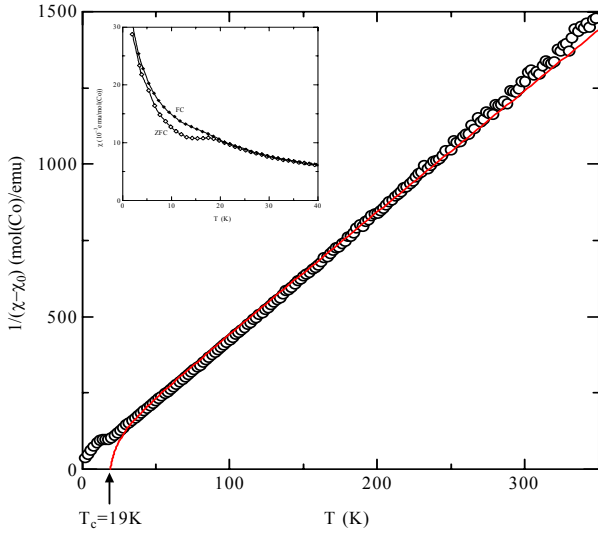|	$x = 0$	$x = 0.01$	$x = 0.02$	$x = 0.03$
$\rho(10^{-3}\Omega\text{cm})$	17.3	17.9	16.7	18.1
$R_H(10^{-3}\text{cm}^3/C)$	11.2	11.1	11.3	11.0
$n(10^{20}/\text{cm}^3)$	5.58	5.65	5.52	5.70
$\mu(\text{cm}^2/\text{Vs})$	0.64	0.60	0.66	0.59
$S(10^{-6}\text{V/K})$	119	118	126	119
$S^2/\rho(10^{-4}\text{W/mK}^2)$	0.82	0.78	0.95	0.78
$A(10^{-3}\text{cm}^2/\text{s})$	6.28	-	-	-
$D(\text{g/cm}^3)$	3.2	-	-	-
$C(\text{J/gK})$	0.616	-	-	-
$\kappa_e(\text{W/mK})$	0.04	0.04	0.04	0.04
$\kappa_L(\text{W/mK})$	1.20	-	-	-
ZT	0.020	-	-	-

Fig.5 Temperature dependence of inverse χ for $x = 0.02$.

4. Conclusion

Polycrystalline specimens of $[(\text{Ca}_{1-x}\text{Pb}_x)_2\text{CoO}_{3.1}]_{0.62}\text{CoO}_2$ $(0 \leqq x \leqq 0.03)$ have been prepared using the conventional solid-state reaction method, and the effect of Pb substitution on the TE properties have been studied. The sample with x=0.02 shows rather low ρ and large S suggesting promising TE materials at room temperature. Seebeck and Hall coefficient measurements reveal that the major charge carriers in the samples are holes, however, the carrier concentration does not change with increasing x. The magnetic susceptibility measurements reveal that Pb ions take divalent state in the RS-type BL. The average valence state of Co ions for $x = 0.02$ was determined as 3.14 in CoO_2 sheet and 3.65 in RS-type BL.

References
1. I. Terasaki, Y. Sasago and K. Uchinokura: Phys. Rev. B **56** (1997) R12685.
2. S. Li, R. Funahashi, I. Matsubara, K. Ueda and H. Yamada: J. Mater. Chem. **9** (1999) 1659.
3. A. C. Masset, C. Michel, A. Maignan, M. Hervieu, O. Toulemomde, F. Aruder, B. Raveau and J. Hejtmanek: Phys. Rev. B **62** (2000) 166.
4. Y. Miyazaki, K. Kudo, M. Akoshima, Y. Ono, Y. Koike and T. Kajitani: Jpn. J. Appl. Phys. **39** (2000) L531.
5. S. Lambert, H. Leligny and D. Grebille: J. Solid State Chem. **160** (2001) 322.
6. Y. Miyazaki, M. Onoda, T. Oku, M. Kikuchi, Y. Ishii, Y. Ono, Y. Morii and T. Kajitani: J. Phys. Soc. Jpn. **71** (2002) 491.
7. S. Li, R. Funahashi, I. Matsubara, K. Ueno, S. Sodeoka and H. Yamada: Chem. Mater. **12** (2000) 2424.
8. R. Funahashi, I. Matsubara, H. Ikuta, T. Takeuchi, U. Mizutani and S. Sodeoka: Jpn. J. Appl. Phys. **39** (2000) L1127.
9. J. Shimoyama, S. Horii, K. Otzschi, M. Sano and K. Kishio: Jpn. J. Appl. Phys. **42** (2003) L194.
10. K. Ohoyama, T. Kanouchi, K. Nemoto, M. Ohashi, T. Kajitani and Y. Yamaguchi: Jpn. J. Appl. Phys. **37** (1998) 3319.
11. A.Yamamoto: Acta Cryst. A **49** (1993) 831.
12. J. Sugiyama, H. Itahara, T. Tani, J. H. Brewer and E. J. Ansaldo: Phys. Rev. B **66** (2002) 134413.
13. W. Koshibae, K. Tsutsui and S. Maekawa: Phys. Rev. B **62** (2000) 6869.
14. K. Takahata, Y. Iguchi, T. Itoh, D. Tanaka and I. Terasaki: Phys. Rev. B **61** (2000) 12551.
15. R. D. Shannon: Acta Cryst. A **32** (1976) 751.
16. C. Kittel: in *Introduction to Solid State Physics* (John Wiley & Sons, NY, 1996) 7th ed, p. 461.
17. R. Ray, A. Ghoshray, K. Ghoshray and S. Nakamura: Phys. Rev. B **59** (1999) 9454.